Electron proton instability in the CSNS ring*

WANG Na(王娜)[1)] QIN Qing(秦庆) LIU Yu-Dong(刘瑜冬)

(Institute of High Energy Physics, CAS, Beijing 100049, China)

Abstract The electron proton (e-p) instability has been observed in many proton accelerators. It will induce transverse beam size blow-up, cause beam loss and restrict the machine performance. Much research work has been done on the causes, dynamics and cures of this instability. A simulation code is developed to study the e-p instability in the ring of the China Spallation Neutron Source (CSNS).

Key words electron cloud, instability

PACS 29.27.Bd, 29.20.dk

1 Introduction

The electron proton instability has been considered as one of the potential threats in the proton rings[1, 2]. CSNS[3] is a proton accelerator facility with consists of a linac and a rapid cycling synchrotron (RCS). Two bunches with a population of 1.88×10^{13} will be accumulated and accelerated in the RCS ring, and the electron-proton instabilities might happen in such high intensity proton ring. A code[4] investigating the electron cloud instability in the position ring is upgraded to study the electron proton instability in the proton ring. In this article, we first discuss the electron cloud build-up in the vacuum chamber, and then give a brief introduction of the physical model used in the simulation. After that, the simulation result of the electron proton interaction will be discussed. Finally, we make a summary of the whole investigation.

The main parameters of the RCS ring are summarized in Table 1.

Table 1. Main parameters of the RCS ring.

parameters	symbol, unit	value
inj./Ext. Energy	$E_{\rm in}/E_{\rm ext}$, GeV	0.08/1.6
circumference	C, m	230.8
bunch population	$N_{\rm p}$, $\times10^{12}$	9.4
number of bunches	$n_{\rm b}$	2
harmonic number	H	2
beam pipe radii	a/b, mm	110/110
e^- prod. rate(proton loss)	$Y_{\rm bl}$, e^-/p/turn	1.16×10^{-2}
e^- prod. rate(ionization)	$Y_{\rm ion}$,e^-/p/turn	1.22×10^{-5}
max secondary e^- yield	$\delta_{\rm max}$	2.1
incident e^- energy at $\delta_{\rm max}$	$E_{\rm max}$, eV	250

2 Electron cloud build-up

The electron cloud density in the vacuum chamber which depends both on the property of the beam pipe environment and the beam itself. Three candidate mechanisms of electron production are considered in this article, including: lost protons hitting on the chamber wall, electrons produced by residual gas ionization, and secondary electron emission.

The electron yield due to residual gas ionization is determined by the ionization cross section and the vacuum pressure in the beam chamber[5]. Residual gases of CO and H_2 are considered, whose ionization cross sections are $\sigma(\rm CO)=1.3\times10^{-22}$ m^2 and $\sigma(\rm H_2)=0.3\times10^{-22}$ m^2. The corresponding electron yield at vacuum pressure $p=10$ nTorr and room temperature ($T=294$ K) is 1.22×10^{-5} e^-/p/turn. The electrons are produced along the beam trajectory.

The mechanism of electron yield due to proton loss is not yet well known. In the simulation, we use the simplified model proposed by Furman et al[6], that the number of electrons generated by lost protons hitting the vacuum chamber wall is $N_{\rm p}\times Y\times p_{\rm loss}$

Received 6 January 2009

* Supported by NSFC (10725525, 10605032)

1) E-mail: wangn@ihep.ac.cn

per turn for the whole ring, where Y is the effective electron yield per lost proton, and $p_{\rm loss}$ is the proton loss rate per turn per beam particle. According to the beam loss tracking simulation of the RCS ring[7], a total beam loss of 6% mostly occurs in the collimation region during the first 1 ms. By using the assumption of 100 e^-/p/loss[6], we obtain an electron production rate of 1.16×10^{-2} per turn, which is 3 orders higher than that of gas ionization. We assume the lost proton time distribution to be proportional to the longitudinal bunch intensity.

Another important origin of electrons is the secondary electron emission due to electron multipacting on the chamber wall. The secondary electron yield, δ, is expressed by[8]

$$\delta(E_{\rm r},\theta)\approx\delta_{\rm max}1.11(E_{\rm r})^{-0.35}(1-{\rm e}^{-2.3E_{\rm r}^{1.35}})/\cos\theta\,, \quad (1)$$

where θ is the incident angle, $\delta_{\rm max}$ the max secondary electron yield, $E_{\rm r}=E_0/E_{\rm max}$, E_0 the incident electron energy and $E_{\rm max}$ the incident electron energy at $\delta_{\rm max}$. Here we use the typical stainless steel SEY parameters in the following calculation.

3 Physical model

The RCS ring stores two bunches with long gaps of tens of meters. The current density profile is shown in Fig. 1. In our simulation we assume the beam has uniform distribution with radius $r = 35$ mm in the transverse plane, and we use the simulated result of painting injection for the longitudinal intensity profile[7]. The vacuum chamber in the simulation is considered as perfectly conducting pipe with circular cross section. As the bunches are about several tens of meters in length, the bunches are longitudinally sliced that each slice has an equal number of particles. The long bunch gaps are also divided into intermediate steps to calculate the electron motion and secondary electron emission. Due to the longitudinal movement, the particles in different slices are rearranged after each bunch passage according to their longitudinal position. The energy ramping of the bunches is considered during each turn, and the curves of acceleration RF voltage and RF phase obtained in Ref. [7] are used.

The electrons are simulated by macro particles. We use 1000 macroparticles to represent primary electrons generated when each bunch slice passes through the electron region. The secondary electron emission occurs when the particles hit on the beam chamber wall. The macro electrons are tracked dynamically in the transverse plane. The space charge force is computed by using PIC method, and applied to particles at each slice in the bunch and each step in the gap. The motion of macro-electrons and macro-protons are tracked during the EC region. After that, the bunch is transformed according to the six-dimensional linear transfer matrix.

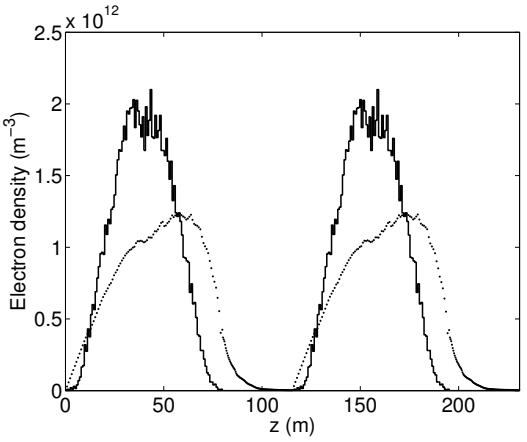

Fig. 1. Build-up of the electron cloud.

4 Simulation results

The build-up of the electron cloud during the passage of the beam is shown in Fig. 1. The dark line shows the current density profile of the beam with arbitrary units, and the dotted line shows the electron density evolution during the bunch passage. The electron cloud density has a fast increase during the passage of the front edge of the bunch, and saturates around the flat top of the profile. When the bunch intensity decreases to a certain extent during the passage of the bunch tail, the electron density begins to fall.

This phenomena can be explained by the fact that the average energy of the electrons hitting the wall is around 30 eV according to the simulation, and hence the SEY is smaller than 1. So the electrons will be absorbed when hitting on the wall equivalently. In the front edge of the bunch profile, the population of electrons is still low, and the increase of the electron density is dominated by the generation of primary electrons. As the number of electrons increase, more and more electrons will be absorbed because of hitting on the chamber wall, and thus the growth of the electron density slows down. When the generation and absorption of electrons equal, the electron density reaches a peak value. Afterward, the electron density goes down due to the decrease of the electron production rate of proton loss, as it is proportional to the bunch current density. During the bunch gap, the average energy of electrons decreases because of

multi pacting effect, and then the beam pipe act as a net absorber to electrons. Fig. 2 presents the electron density evolution during the passage of the first twenty bunches.

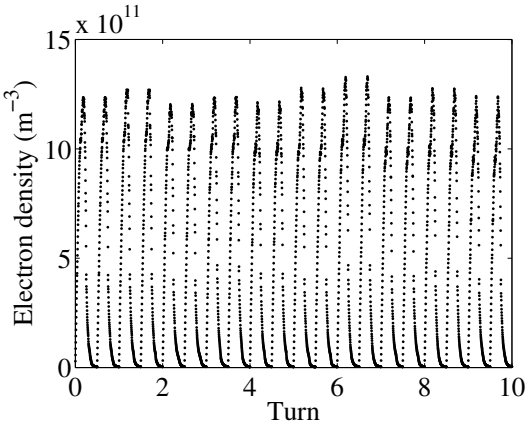

Fig. 2. Electron density evolution during the passage of the first twenty bunches.

We also evaluated the effects of several significant parameters on the electron cloud formation. We vary the electron production rate of proton loss from 1.16×10^{-2} to 1.16×10^{-1} e^-/p/turn, and the electron cloud build-up during the first few bunch passages is shown in Fig. 3. We can see that the peak densities of different cases are almost proportional to the proton loss rate, which demonstrates the dominant role of proton loss in the electron cloud generation.

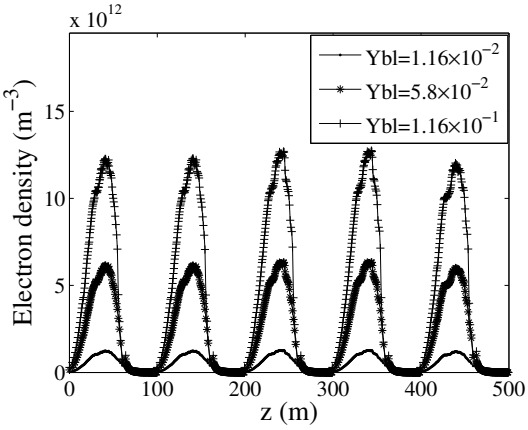

Fig. 3. Build-up of the electron cloud for different electron production rates.

We find that the changes of maximum secondary electron yield from 1.1 to 2.1 have not made significant difference on the saturated electron density as expected. This can be explained by the fact that the secondary electron production rate SEY, corresponding to the average energy of electrons hitting on the wall, is smaller than 1, and the electrons generated by the proton loss on walls is the dominant origin of electron cloud formation. In addition, significant changes in the vacuum pressure have little effect on the electron cloud formation.

In order to study the beam instability caused by the electron cloud, we tracked the beam for about one hundred turns and recorded the centroid position and transverse rms size of the slices. The simulation results show that there is no beam size blow-up or excitation of serious transverse centroid oscillation during the interaction of the electron and proton beams. We ascribe this to the long gap between the bunches. But further investigation is needed on the instability threshold and growth rate.

5 Summary

A simulation code is developed to study the electron proton interaction in the RCS ring. Primary simulation results of electron cloud build-up and electron cloud induced instability have been given.

The mechanisms of electron yield due to proton loss, gas ionization and secondary emission have been considered in the simulation. Primary electrons are generated at the surface of the chamber wall or beam trajectory. As the bunch gap is sufficient long, the electron cloud will not accumulate during successive bunch passages. We have also studied the effects of different parameters on the electron cloud build-up, and found that the electrons generated by proton loss on the walls play the dominant role during the electron cloud formation. Significant changes in the production rate of ionization electrons or secondary electron yield have little effect on the electron density evolution.

The preliminary simulation on electron proton instability shows that this kind of instability may not be strong enough to cause serious problem in the RCS ring. But more work should be done on the analysis of the instability threshold and the frequency spectrum.

In this article, we assume the lost protons are uniformly distributed in separate turns during the first 1 ms. However, large proton loss may happen during certain turns in the real situation. In addition, electron build-up during the injection process has been excluded, which may also bring serious beam stability problems. These subjects should be further studied. As the proton loss is the main source of the electron yield, we still should restrict the proton loss to a certain level in order to control the build-up of electron cloud.

The authors would like to thank the members of

the CSNS Accelerator Physics Group. Special thanks go to T. Wei for valuable discussion on the initial particle distribution and proton loss along the ring.

References

1 Ohmi K, Toyama T, Ohmori C. Phys. Rev. ST Accel. Beams, 2002, **5**: 114402

2 Pivi M, Furman M A. Electron-colud update simulation results for the PSR, and recent results for the SNS. In: Garvey T et al. Proceedings of EPAC'02. Paris, France: EPS-IGA and CERN, 2002. 1547—1549

3 WEI Jie, FU Shi-Nian, FANG Shou-Xian et al. China Spallation Neutron Source Accelerators: Design, Research, and Development. In: C. Biscari et al. Proceedings of EPAC'06. Edinburgh, Scotland: EPS-AG, 2006. 366—368

4 LIU Tu-Dong, GUO Zhi-Yuan, QIN Qing et al. HEP & NP, 2004, **28**: 1222—1226 (in Chinese)

5 Furman M A, Lambertson G R. LBNL Report No. LBNL-41123, 1997

6 Furman M A, Pivi M. Simulation Results for the Electron-Cloud at the PSR. In: Lucas P, Webber S. Proceedings of PAC'01. Chicago, U.S.A.: IEEE, Inc, 2001. 707—709

7 WEI Tao, FU Shi-Nian, QIN Qing et al. Chinese Physics C, 2008, **32**: 437—441

8 Seiler H. J. Appl. Phys., 1983, **54**: R1-R18